Earth and Planetary Science Letters 533 (2020) 116055

Contents lists available at ScienceDirect

Earth and Planetary Science Letters

www.elsevier.com/locate/epsl

I/Ca in epifaunal benthic foraminifera: A semi-quantitative proxy for bottom water oxygen in a multi-proxy compilation for glacial ocean deoxygenation

Wanyi Lu [a], Rosalind E.M. Rickaby [b], Babette A.A. Hoogakker [c], Anthony E. Rathburn [d], Ashley M. Burkett [e], Alexander J. Dickson [f], Gema Martínez-Méndez [g,h], Claus-Dieter Hillenbrand [i], Xiaoli Zhou [j], Ellen Thomas [k,l], Zunli Lu [a,*]

[a] Department of Earth Sciences, Syracuse University, Syracuse, NY, USA
[b] Department of Earth Sciences, University of Oxford, Oxford, UK
[c] The Lyell Center, Heriot-Watt University, Edinburgh, UK
[d] Department of Geological Sciences, California State University, Bakersfield, CA, USA
[e] Boone Pickens School of Geology, Oklahoma State University, Stillwater, OK, USA
[f] Department of Earth Sciences, Royal Holloway University of London, Egham, UK
[g] MARUM – Center for Marine Environmental Sciences, University of Bremen, Bremen, Germany
[h] Alfred Wegener Institute, Helmholtz Centre for Polar and Marine Research, Germany
[i] British Antarctic Survey, Cambridge, UK
[j] Department of Marine and Coastal Sciences, Rutgers University, New Brunswick, NJ, USA
[k] Department of Geology and Geophysics, Yale University, New Haven, CT, USA
[l] Department of Earth and Environmental Sciences, Wesleyan University, Middletown, CT, USA

ARTICLE INFO

Article history:
Received 14 June 2019
Received in revised form 18 December 2019
Accepted 27 December 2019
Available online xxxx
Editor: L. Robinson

Keywords:
I/Ca
benthic foraminifera
Cibicidoides spp.
bottom water oxygen
glacial-interglacial cycles

ABSTRACT

The decline in dissolved oxygen in global oceans (ocean deoxygenation) is a potential consequence of global warming which may have important impacts on ocean biogeochemistry and marine ecosystems. Current climate models do not agree on the trajectory of future deoxygenation on different timescales, in part due to uncertainties in the complex, linked effects of changes in ocean circulation, productivity and organic matter respiration. More (semi-)quantitative reconstructions of oceanic oxygen levels over the Pleistocene glacial cycles may provide a critical test of our mechanistic understanding of the response of oceanic oxygenation to climate change. Even the most promising proxies for bottom water oxygen (BWO) have limitations, which calls for new proxy development and a multi-proxy compilation to evaluate glacial ocean oxygenation. We use Holocene benthic foraminifera to explore I/Ca in *Cibicidoides* spp. as a BWO proxy. We propose that low I/Ca (e.g., <3 μmol/mol) in conjunction with benthic foraminiferal carbon isotope gradients and/or the surface pore area percentages in foraminiferal tests (e.g., >15%) may provide semi-quantitative estimates of low BWO in past oceans (e.g., <∼50 μmol/kg). We present I/Ca records in five cores and a global compilation of multiproxy data, indicating that bottom waters were generally less-oxygenated during glacial periods, with low O_2 waters (<∼50 μmol/kg) occupying some parts of the Atlantic and Pacific Oceans. Water mass ventilation and circulation may have been important in deoxygenation of the glacial deep Pacific and South Atlantic, whereas enhanced remineralization of organic matter may have had a greater impact on reducing the oxygen content of the interior Atlantic Ocean.

1. Introduction

Observations and climate models show increased ocean deoxygenation as a response to global warming, due to decreased oxygen solubility in warmer waters combined with decreased ventilation of the deep ocean due to increased thermal stratification (Breitburg et al., 2018; Keeling et al., 2009; Schmidtko et al., 2017), and a decrease in the lateral advection of oxygenated waters (Gruber et al., 2001). However, current climate models tend to underestimate spatial oxygen variability and temporal trends (Oschlies et al., 2017; Stramma et al., 2012), partially due to an inability to pre-

* Corresponding author.
E-mail address: zunlilu@syr.edu (Z. Lu).

https://doi.org/10.1016/j.epsl.2019.116055
0012-821X/

cisely tease apart contributions to deoxygenation from three main controls: (i) temperature related oxygen solubility; (ii) ventilation of water masses and other physical processes; (iii) biogeochemical processes (e.g., biological production and respiration) (Oschlies et al., 2018). Models tend to agree on (i), but disagree on (ii) and (iii), which leads to different projections of expanding vs. shrinking oxygen minimum zones (OMZ) over the long-term future (Resplandy, 2018).

Geological records commonly link ocean deoxygenation to greenhouse climates (e.g., Jenkyns (2010); Penn et al. (2018)), but deoxygenation also occurred during cold periods in deep time (e.g., at the Late Ordovician – Early Silurian (Bartlett et al., 2018) and across the Frasnian – Famennian boundary (Song et al., 2017)). Thus, temperature alone does not dictate ocean deoxygenation, indicating that we need a better understanding of the interplay between physical and biogeochemical processes during climate change.

Deoxygenation was common during Pleistocene glacials (e.g., Bradtmiller et al. (2010); de la Fuente et al. (2017); Gottschalk et al. (2016a); Hoogakker et al. (2015, 2018); Jaccard et al. (2016); Jacobel et al. (2020); Loveley et al. (2017); Umling and Thunell (2018)), and there is much evidence that global deep oceans (>2 km) were less-oxygenated during the Last Glacial Maximum (LGM, 18-22 ka) than in the early Holocene (Jaccard and Galbraith, 2012). However, this evidence is generally qualitative (Jaccard and Galbraith, 2012), and quantitative O_2 estimates for the glacial oceans are needed to further assess and differentiate drivers for deoxygenation.

Qualitative bottom water oxygen (BWO) proxies traditionally used on glacial-interglacial time scales include sedimentary structures (e.g., lamination due to lack of bioturbation), benthic foraminiferal assemblages and species abundances, and trace metal concentrations (Jaccard and Galbraith, 2012). The authigenic uranium content of sediments (aU, i.e., accumulation of reduced U(IV) in excess of U in detrital sediments) (Bradtmiller et al., 2010; Durand et al., 2018; Jaccard et al., 2016; Jacobel et al., 2017; Loveley et al., 2017) is controlled by BWO and the rain of organic material from surface ocean (which consumes O_2 as it is respired) (Bradtmiller et al., 2010). If sediments become more reducing (higher aU values) with similar or lower export production (no increased O_2 consumption), it can be reliably inferred that higher aU is due to a decrease in BWO. But a lack of high aU values does not preclude deoxygenation: subsequent reoxygenation at the sampling site could obliterate sedimentary aU enrichments that had previously developed (Bradtmiller et al., 2010; Costa et al., 2018; Jacobel et al., 2020). The benthic foraminiferal oxygen index based on species assemblage and morphology data, also used to qualitatively trace BWO (Kaiho, 1994), is poorly supported by calibration with living foraminifera (Jorissen et al., 2007), and the impact of factors other than the BWO level (e.g., organic matter flux) cannot be easily separated from the overall signal.

Four recently developed proxies have promise to provide semi-quantitative constraints on BWO: (1) the pore area in benthic foraminiferal tests (Rathburn et al., 2018), (2) benthic foraminiferal carbon isotope gradients (Hoogakker et al., 2015), (3) preservation of organic compounds (Anderson et al., 2019), (4) and the benthic I/Ca proxy (Glock et al., 2014). We highlight these newly developed BWO proxies because they have been validated/calibrated to various degrees in modern sediments/foraminifera. Furthermore, they show some potential to reconstruct specific BWO values instead of being limited to qualitative reconstruction of higher/lower BWO or increased/decreased extent of suboxic water mass.

The pore area percentage in tests of the epifaunal (on or above the seafloor surface living) benthic foraminifer *Cibicidoides wuellerstorfi* is correlated with BWO in the modern ocean (Rathburn et al., 2018), but this proxy has not yet been tested in down-core studies. Several studies have related pore size of different species of benthic foraminifera to ambient conditions, but most have focused on taxa that live within sediments (infaunal) (e.g., Kuhnt et al. (2014)), and may be influenced by pore water conditions and nitrate respiration (Rathburn et al., 2018).

The benthic foraminiferal carbon isotope gradient ($\Delta\delta^{13}C$) between epifaunal (*C. wuellerstorfi*) and deep infaunal benthic foraminifera species (*Globobulimina* spp.) was quantitatively calibrated to BWO values (20–235 μmol/kg) in a global deep ocean dataset (Hoogakker et al., 2018, 2015; McCorkle and Emerson, 1988). The application of this proxy is limited by the restricted occurrence of these species, with *Globobulimina* spp. requiring relatively high export productivity (Jorissen et al., 2007). In addition, $\delta^{13}C_{C.\ wuellerstorfi}$ may be influenced by seasonal variability in export productivity of labile organic matter to the seafloor, i.e., the phytodetrital flux ('Mackensen effect') (Mackensen et al., 1993); and $\delta^{13}C_{Globobulimina}$ may be affected by isotopically light carbon released by anaerobic processes including denitrification and sulfate reduction, especially in high sediment accumulation environments, thus altering the relationship between $\Delta\delta^{13}C$ and BWO (McCorkle and Emerson, 1988; Jacobel et al., 2020).

Another recently proposed, empirical proxy is the use of the preservation of specific organic compounds (as observed in Arabian Sea sediments) to estimate BWO concentrations in the central Equatorial Pacific (Anderson et al., 2019): an order-of-magnitude greater accumulation of lipid biomarkers (e.g., C_{37} alkenones) combined with evidence for lower export production was argued to indicate a BWO content of 20–50 μmol/kg, although uncertainty remains about the mechanism of organic matter preservation (Hedges and Keil, 1995) and the validity of applying this empirical relationship based on Arabian Sea data to other regions (Anderson et al., 2019).

The carbonate I/Ca proxy has been applied across different time scales, and can be used to resolve subtle changes in oceanic oxygenation (Lu et al., 2018, 2016). Iodate ($[IO_3^-]$, oxidized form) and iodide ($[I^-]$, reduced form) are the thermodynamically stable forms of iodine in seawater (Wong and Brewer, 1977); $[IO_3^-]$ is completely reduced to $[I^-]$ in anoxic environments (Rue et al., 1997). $[IO_3^-]$ is the only iodine species incorporated into carbonate (Lu et al., 2010) by replacing $[CO_3^{2-}]$ (Feng and Redfern, 2018; Podder et al., 2017), thus lower foraminiferal I/Ca generally records more O_2-depleted conditions (Lu et al., 2016).

Modern BWO concentrations at low ranges (2–34 μmol/kg) correlate with I/Ca in infaunal and epifaunal living foraminifera (Glock et al., 2014). To date, only one calcitic epifaunal species, *Planulina limbata*, has been analyzed for its I/Ca in modern settings (Glock et al., 2014), documenting impingement of an OMZ on the seafloor. *Cibicidoides* spp. are more commonly used in paleoceanographic investigations, and thus I/Ca in cosmopolitan *Cibicidoides* species may have great potential as a BWO proxy for comparison with proxy data for other paleoenvironmental parameters. *Cibicidoides wuellerstorfi* and *C. lobatulus* are typically attached to objects projecting 0–2 cm above the sediment-water interface (Lutze and Thiel, 1989; Rathburn and Corliss, 1994; Schweizer et al., 2009). Other *Cibicidoides* spp. (e.g., *C. mundulus*, *C. pachyderma*) may live in the top 2 cm of the sediment, and can adapt from an epifaunal (bottom water exposure) to a shallow infaunal (pore water exposure) habitat (Wollenburg et al., 2018). *Cibicidoides* spp. are generally not abundant in low O_2 waters (Jorissen et al., 2007), but *C. wuellerstorfi* has been observed living in settings with O_2<50 μmol/kg (Rathburn et al., 2018; Venturelli et al., 2018).

Here we report a global *Cibicidoides* spp. I/Ca data set obtained from living (i.e., Rose Bengal stained and live-picked) and unstained (i.e., living and dead) benthic foraminifera tests in core-top sediments of Holocene-modern age. The intention is to characterize benthic I/Ca relative to modern BWO values. We combine I/Ca

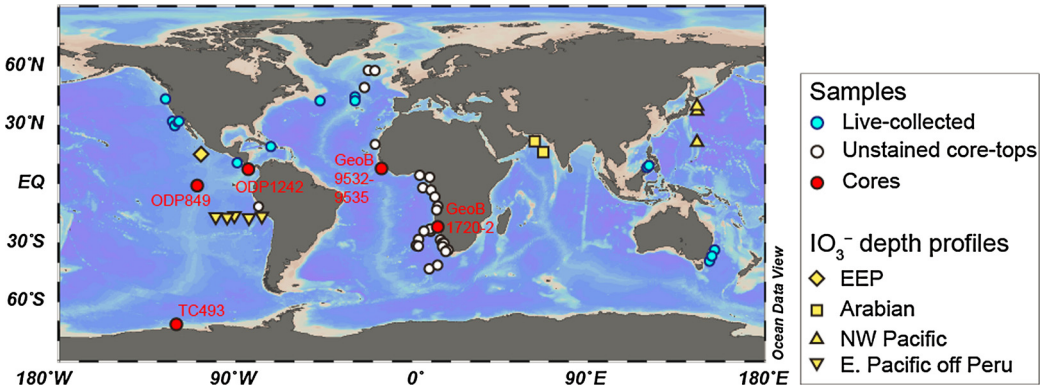

Fig. 1. Core and sample locations (EEP: Eastern Equatorial Pacific).

with $\Delta\delta^{13}C$ and surface pore area values to explore how these proxies may be combined to provide more reliable (semi-)quantitative BWO estimates. We then estimate bottom water oxygenation changes in glacial oceans from five down-core I/Ca records, and integrate these with an updated global compilation of independent oxygenation proxies ($\Delta\delta^{13}C$, aU, and C_{37} alkenones) to explore a broader pattern of glacial BWO conditions. We do not strictly focus on the LGM in the I/Ca records because the temporal resolution of some records is relatively low, but focus instead on more broadly defined glacial periods, i.e., Marine Isotope Stages (MIS) 2–4 and 6.

2. Materials and methods

2.1. Materials

For sampling locations of live-collected and unstained core-top foraminifera and core sites, see Fig. 1 and Table S1. Foraminifera were either collected alive onboard ship (living attached on the hard surfaces such as rocks, worm tubes or artificial substrates, and manually removed), or stained with Rose Bengal and determined to have been alive at the time of collection using conservative assessments (Rathburn et al., 2018). The living foraminifera were imaged using Scanning Electron Microscopy to determine the areal percentage of pores in their tests (Rathburn et al., 2018), then cleaned and dissolved to analyze the I/Ca of their tests.

Unstained foraminifera from core-top sediments contain both living and dead foraminifera. Gravity or piston cores may lose some seafloor surface sediments, and core-tops from such cores are likely to contain a higher percentage of dead foraminifera (Rathburn and Miao, 1995). Multicorer surface sediments are more likely to include the living population along with dead foraminifera. The living population represents conditions at the time of collection, whereas the dead assemblage (and living plus dead) may contain a different suite of species, including these living at the location in the recent and more distant past, depending on bioturbation and taphonomic processes (Loubere and Gary, 1990). Radiocarbon and $\delta^{18}O$ values of selected core-top samples in this study reveal Holocene ages (Table S1).

2.2. Age models

We show five down-core I/Ca records: ODP Site 1242 (7.86°N, 83.61°W, 1400 m); ODP Site 849 (0.18°N, 110.50°W, 3800 m); TC493 (71.15°S, 119.92°W, 2096 m); GeoB1720-2 (28.98°S, 13.83°E, 1997 m), and GeoB9532-9535 (8.90°N, 14.90°W, 319-667 m) (Table S2). Age models for ODP Site 1242 and ODP Site 849 are after Hoogakker et al. (2018), core TC493 is after Lu et al. (2016), core GeoB1720-2 is after Dickson et al. (2009); Lu et al. (2019), and GeoB9532-9535 is after Huang et al. (2012).

2.3. Foraminiferal I/Ca analyses

Benthic foraminiferal I/Ca was measured following the method for planktic foraminiferal I/Ca (Lu et al., 2016). For each sample, 3–15 specimens from >250 μm size fraction were used depending on foraminifera availability. The foraminifera were gently crushed between two clean glass plates to open the chambers, then cleaned following the Mg/Ca protocol (Barker et al., 2003). Crushed foraminiferal shells were ultra-sonicated in water to remove clays. NaOH-buffered H_2O_2 was then added, and the sample was kept in boiling water for 10–20 mins to remove organic matter. Reductive cleaning was not applied, as the effects of Mn oxide coatings on I/Ca signal are minimal (Zhou et al., 2014). After thorough rinsing, samples were dissolved in 3% HNO_3, then mixed with a matrix containing internal standard and buffered by tertiary amine. Iodine and calcium concentrations were measured by quadrupole ICP-MS (Bruker M90) at Syracuse University. Calibration standards were freshly made for each batch of samples. The 1 ppb iodine signal was tuned to >80 kcps. The reference material JCp-1 was measured repeatedly to maintain long-term accuracy (Lu et al., 2010). The standard deviation for each measurement was usually lower than 1%. Replicates of selected *C. wuellerstorfi* from core GeoB1720-2 show reproducibility ranging from ±2% (0.07 μmol/mol; 1σ) to ±9% (0.23 μmol/mol; 1σ) for I/Ca (Table S2).

2.4. O_2 data

The O_2 data for sample sites of living foraminifera are *in-situ* bottom water O_2 data after Rathburn et al. (2018). They were determined measuring high-resolution oxygen profiles from the overlying water into the sediment in multi-corer tubes taken at the collection site, using amperometric oxygen microelectrodes, or an oxygen sensor mounted on a CTD or submersible. For unstained core-top samples, *in-situ* O_2 data are not available, and we used O_2 data from the Electronic Atlas of the World Ocean Circulation Experiment (http://www.ewoce.org/). For core-top samples located in coastal areas in the Southeast Atlantic, we used O_2 data from the nearest site from the World Ocean Database 2013 (https://www.nodc.noaa.gov/OC5/WOD13/) (Boyer et al., 2013) because of the greater spatial variability in O_2 conditions in this region.

3. Results

I/Ca in shells of living and unstained foraminifera from core-top sediments decreases with lower BWO, except for the middle O_2 range (50–200 μmol/kg) (Fig. 2). Furthermore, benthic I/Ca does not appear to decrease gradually across the entire oxygenation spectrum from oxic (BWO > 70 μmol/kg), hypoxic (BWO < 70 μmol/kg), suboxic (BWO < 10 μmol/kg) to anoxic (no O_2)

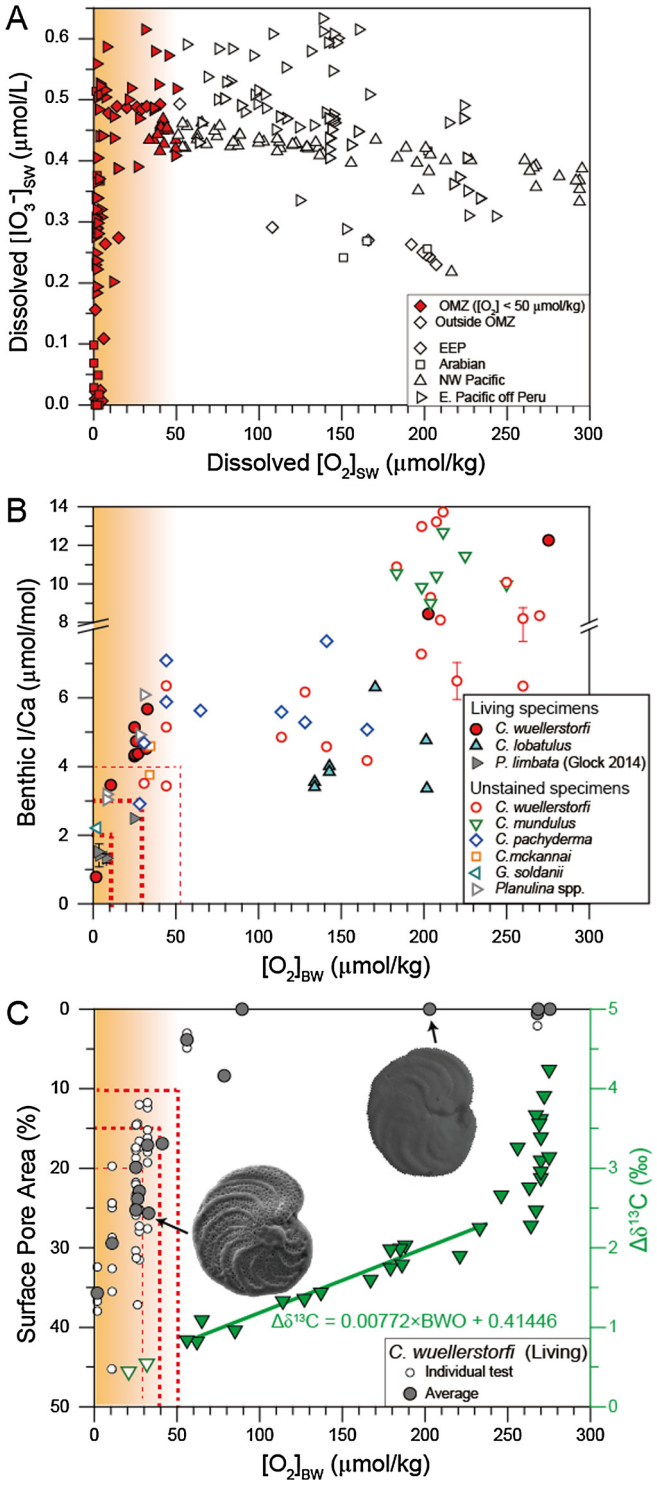

Fig. 2. (A). Dissolved oxygen concentration ($[O_2]_{SW}$) versus dissolved iodate concentration in seawater ($[IO_3^-]_{SW}$) (Cutter et al., 2018; Farrenkopf and Luther, 2002; Huang et al., 2005; Rue et al., 1997). (B). I/Ca in shells of living and unstained benthic foraminifera from core-top sediments versus bottom water oxygen concentrations ($[O_2]_{BW}$). Error bars for y axis indicate the s.d. (1 s.d.) of duplicate measurements. (C). Surface pore areas in foraminiferal tests versus ambient $[O_2]_{BW}$ modified from Rathburn et al. (2018); $\Delta\delta^{13}C$ versus $[O_2]_{BW}$ modified from Hoogakker et al. (2015), and two open symbols are from Hoogakker et al. (2018). The orange shading in A, B and C marks $[O_2]$<~50 µmol/kg. The dashed lines in B and C illustrate the I/Ca or pore area cut-off values and related optimal O_2 thresholds determined from the ROC method (for details see text). Thick dashed lines denote AUC > 0.95 (better ROC test results), and the thin dashed lines denote AUC < 0.95. (For interpretation of the colors in the figure(s), the reader is referred to the web version of this article.)

conditions. Instead, benthic I/Ca decreases rapidly below a BWO threshold (e.g., <~50 µmol/kg). In general, low benthic I/Ca are consistent with low BWO, but depending on the thresholds (definition of "low"), low BWO may not exclusively produce low benthic I/Ca. Lower I/Ca values in the tests of *C. wuellerstorfi* correlate significantly with greater surface pore percentages, a proxy for oxygenation (Rathburn et al., 2018), as measured on the same set of specimens ($R^2 = 0.83$, $p < 0.01$) (Fig. 2B-C).

In our five cores from the Eastern Equatorial Pacific (EEP), South Atlantic and Southern Oceans (Fig. 3 and 4, Table S2), low I/Ca values are generally found in glacial samples than in modern/late Holocene samples. At ODP Site 1242 (EEP) and core sites GeoB1720-2 and GeoB9532-9535 (Atlantic), the I/Ca values were close to or less than 3 µmol/mol during parts of the last glacial period. ODP Site 849 (EEP) shows I/Ca between 2.9 and 4.9 µmol/mol throughout the last 150 ka, without pronounced trends. Core TC493 from the Southern Ocean does not have enough *Cibicidoides* spp. specimens in MIS 2 sediments for I/Ca analyses. Where specimens could be found, the corresponding I/Ca values were relatively higher than in the other studied cores. *C. wuellerstorfi* I/Ca was ~6 µmol/mol during glacial MIS 6, increasing to ~12 µmol/mol during interglacial MIS 5e, and *C. lobatulus* I/Ca was ~10 µmol/mol during MIS 6, increasing to ~18 µmol/mol during MIS 5e.

4. Discussion: proxy development

4.1. Epifaunal I/Ca as a semi-quantitative O_2 proxy

The results from living and unstained foraminifera from core-top sediments confirm that low benthic I/Ca values indicate low BWO (Fig. 2). Epifaunal I/Ca does not linearly correlate with BWO, thus I/Ca cannot be calibrated as a quantitative proxy. However, low I/Ca values in epifaunal benthic foraminifera may be used to determine BWO above/below a threshold value as a semi-quantitative proxy. Such a semi-quantitative proxy can be valuable for tuning ocean models at locations, where fully quantitative proxies are not applicable (e.g., where *Globobulimina* spp. are absent).

We apply the statistical method "receiver operating characteristic" (ROC) (Zou et al., 2007) to determine the O_2 threshold for several cut-off values in I/Ca (see Fig. S1 for an example of the statistical results). The statistical results show that lower I/Ca cut-off values generally lead to lower O_2 threshold values (Fig. 2B). A parameter called the area under curve (AUC) describes how well the optimal O_2 threshold separates the two groups of high vs. low I/Ca in these ROC tests. The O_2 threshold values producing a high AUC (>0.95) and good separations are shown by thick dashed lines (Fig. 2B). Similar ROC tests were performed on the surface pore area data (Fig. 2C). These statistically optimal O_2 thresholds are influenced by the choice of cut-off value and available calibration dataset. For example, using only the living specimen dataset (a smaller calibration dataset), the ROC analyses show a slightly different optimal O_2 threshold for the same I/Ca cut-off value. Adding more I/Ca and surface pore area data in the O_2 < 50 µmol/kg window will very likely change the statistically-determined O_2 threshold value.

These statistically-determined O_2 threshold values must be viewed with caution in the context of a multi-proxy approach (see section 4.2): pore area percentages start to increase notably below 50 µmol/kg, and $\Delta\delta^{13}C$ has not yet been fully calibrated below 50 µmol/kg (Fig. 2C). Thus BWO of ~50 µmol/kg could be an important target for ocean biogeochemical models and carbon cycle models. Proposing a lower O_2 threshold value may lead to overestimate the degree of deoxygenation in down-core studies. For now, we propose that *Cibicidoides* spp. I/Ca < 3 µmol/mol in specimens with high pore density (i.e., >15%) may be indicative of

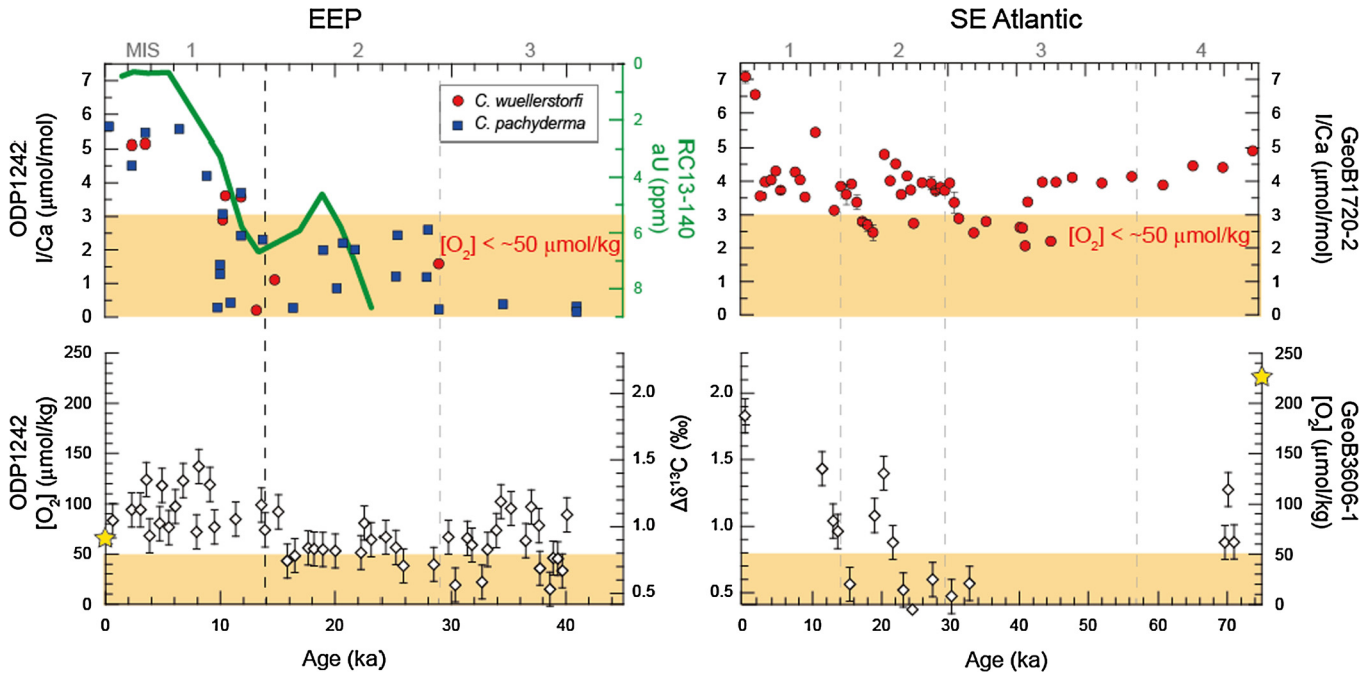

Fig. 3. Comparison of epifaunal I/Ca with O_2 reconstructions from $\Delta\delta^{13}C$ in the EEP (Hoogakker et al., 2018) and Southeast Atlantic (McKay et al., 2016) over the last 45 ka and 75 ka, respectively. The aU record at site RC13-140 is from Bradtmiller et al. (2010). Yellow asterisks in the bottom panels denote the modern bottom water O_2 at the sites.

BWO < ~50 µmol/kg (Fig. 2). Future studies may more rigorously define the O_2 threshold for both I/Ca and pore density.

The attempt to infer BWO from benthic I/Ca values in the low O_2 range (<50 µmol/kg) currently remains empirical, with several limitations. *C. wuellerstorfi* generally are not abundant at low BWO, making it challenging to tightly constrain the threshold O_2 value at which IO_3^- in seawater is reduced and its associated I/Ca in calcite drops (Fig. 2B). In the water column, the O_2 threshold values and kinetics are not completely resolved for either iodate reduction or iodide oxidation (Chance et al., 2014). Paired profiles of dissolved O_2 and [IO_3^-] in the water column at OMZ sites in the EEP (Rue et al., 1997), Arabian Sea (Farrenkopf and Luther, 2002), Northwest Pacific (Huang et al., 2005) and Eastern Pacific off Peru (Cutter et al., 2018) demonstrate that rapid iodate reduction, with a lifetime of ~50 nM per hour (Chance et al., 2014), occurs at O_2 < 20 µmol/kg (Fig. 2A). Such studies are sparse, however, and there are no controlled laboratory experiments in seawater constraining the O_2 threshold of iodate reduction. Coupled seawater chemistry (iodine speciation and BWO) and living specimen I/Ca measurements at the same location may be required to precisely quantify the relationship between epifaunal I/Ca and BWO.

Our set of live-collected and core-top samples was selected to calibrate benthic I/Ca across a wide range of O_2 concentrations (2–270 µmol/kg), but other environmental parameters (such as temperature and water depths) are generally correlated with O_2 in these samples, making it difficult to deconvolve the relations between non-O_2 parameters and I/Ca. For example, we observe a weak correlation between bottom water temperature and benthic I/Ca in living *C. wuellerstorfi* ($R^2 = 0.14$, $p = 0.26$), and a slightly positive correlation in unstained *C. wuellerstorfi* ($R^2 = 0.16$, $p = 0.05$). These correlations cannot be convincingly attributed to a potential temperature effect, because temperature is significantly correlated with BWO ($R^2 = 0.55$, $p < 0.01$). Further core-top studies are required to test non-O_2 effects on I/Ca, under similar O_2 conditions but under a broad range of temperature, salinity, water depths, etc.

4.2. Downcore proxy comparison

Next, we compare two I/Ca down-core records with quantitative BWO reconstructions from $\Delta\delta^{13}C$ on the same core or a nearby core (Fig. 3). At ODP Site 1242 in the EEP, I/Ca values appear to be consistent between the two species (*C. wuellerstorfi* and *C. pachyderma*), with values <3 µmol/mol (and thus <50 µmol/kg BWO) throughout MIS 3 and MIS 2. The $\Delta\delta^{13}C$ records suggest BWO were ~50 µmol/kg during parts of MIS 3 and throughout MIS 2 (Hoogakker et al., 2018).

In the Southeast Atlantic at Site GeoB1720-2, the *C. wuellerstorfi* I/Ca values show only a few values <3 µmol/mol during late MIS 3 and the LGM. The $\Delta\delta^{13}C$ reconstructions at nearby site GeoB3606-1 (25.47°S, 13.08°E, 1785 m) suggest that BWO values were ~50 µmol/kg during late MIS 3 and the early and late phases of MIS 2 (McKay et al., 2016). Higher resolution and improved age models are necessary to better examine the temporal changes in this region.

The epifaunal I/Ca proxy thus is generally (but not perfectly) consistent with the $\Delta\delta^{13}C$ proxy. The difference between I/Ca (GeoB1720-2) and $\Delta\delta^{13}C$ (GeoB3606-1) in the South Atlantic may be due to the relatively low temporal resolution of the records and different locations at which these two proxies were measured. At ODP Site 1242, values of I/Ca and $\Delta\delta^{13}C$ disagree between 10 ka and 15 ka, disregarding whether BWO was above or below 50 µmol/kg (Fig. 3). This discrepancy could be caused by several possibilities: There are still uncertainties in the behavior of $\Delta\delta^{13}C$ in the low BWO range (Fig. 2C) (Hoogakker et al., 2015). The best preserved *C. wuellerstorfi* specimens were used for $\Delta\delta^{13}C$ measurements and the rest of the specimens was used for I/Ca, thus sample heterogeneity amongst foraminifera from the same depth interval in the sediment may also influence the comparison between these two proxies. Alternatively, iodide oxidation kinetics could be slow, with a lifetime ranging between ~4 nM per year and ~670 nM per year (Chance et al., 2014), implying that waters could have been re-oxygenated before the associated iodide was re-oxidized to iodate. We cannot rule out the possibility that the low I/Ca values between 10–15 ka result from slow recovery of O_2 at some

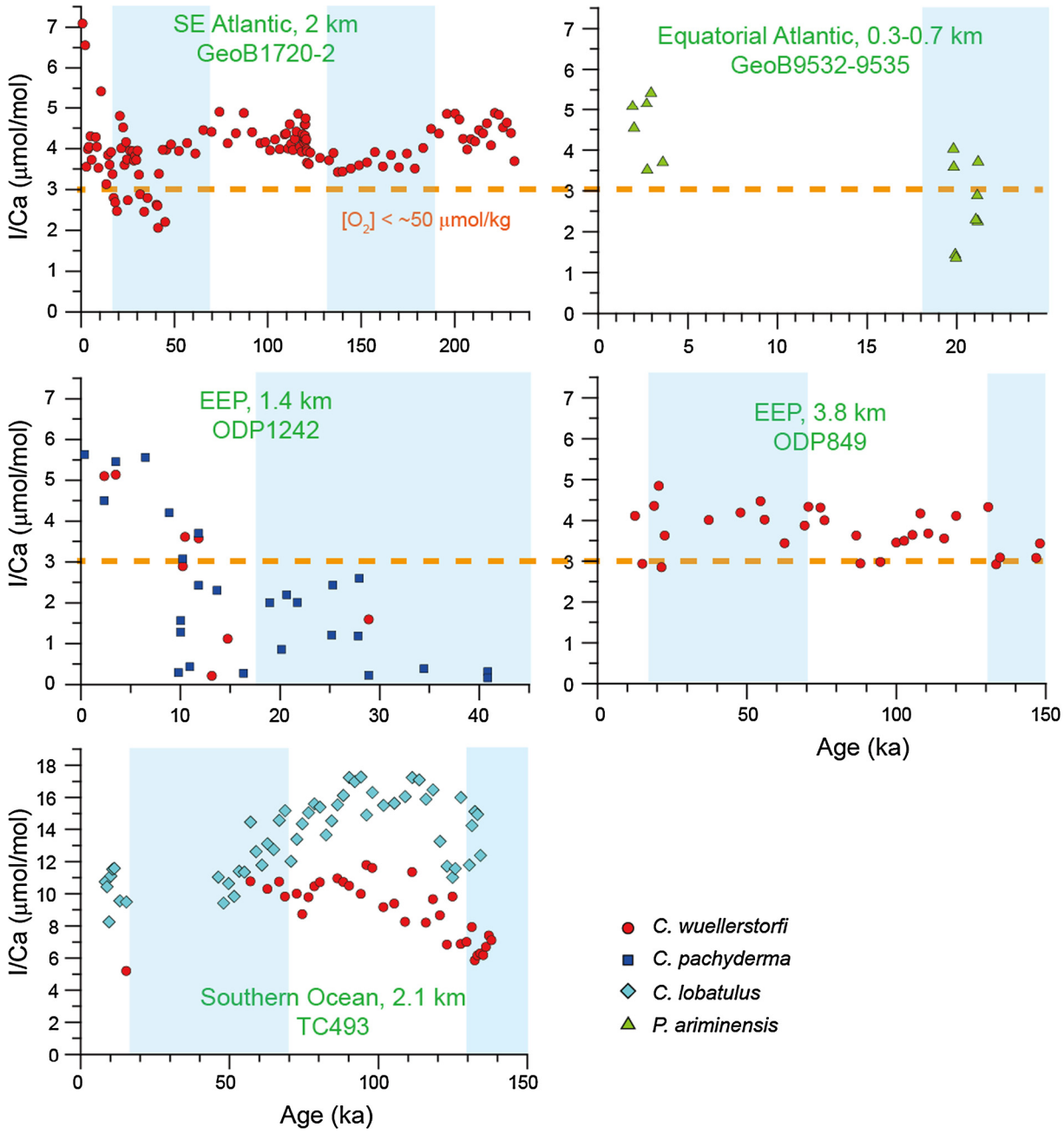

Fig. 4. Down-core records of benthic foraminiferal I/Ca plotted vs. time. Blue shaded areas indicate glacial periods and bold dashed orange lines indicate $[O_2] < \sim 50$ µmol/kg.

"upstream" location, instead of recording *in-situ* BWO at ODP Site 1242. The aU record at nearby site RC13-140 (2.87°N, 87.75°W, 2246 m) shows higher aU concentrations during the period from 10–15 ka than during the Holocene when opal flux was similar/slightly lower (Bradtmiller et al., 2010), suggesting the presence of low BWO water masses from 10–15 ka, similar to the I/Ca trend (Fig. 3).

During the Holocene, the $\Delta\delta^{13}C$ record at ODP Site 1242 shows that BWO first increased from ~80 µmol/kg at 10 ka to a maximum of ~140 µmol/kg at 8 ka, and then decreased to ~80 µmol/kg at modern day. In contrast, the I/Ca values steadily increased from ~3 µmol/mol at 10 ka to ~5 µmol/mol at present day, and aU concentrations steadily decreased from ~3 ppm at 10 ka to 0 ppm at present day. Both I/Ca and aU records can be interpreted qualitatively to reflect lower BWO during the early Holocene compared to modern day; however we cannot infer any reliable BWO values from I/Ca and aU records because *C. wuellerstorfi* I/Ca values were >3 µmol/mol and aU peaks were absent during the late Holocene. It is possible that BWO concentrations at the EEP were fluctuating throughout the Holocene as shown by the $\Delta\delta^{13}C$ record, but this variability cannot be inferred from I/Ca or aU records due to the limitations of these two proxies. Alternatively, the Holocene BWO reconstructions from $\Delta\delta^{13}C$ may be impacted by the incorporation of isotopically light carbon into *Globobulimina* spp. from anaerobic processes (Jacobel et al., 2020).

Epifaunal I/Ca thus can be a useful tool to place semi-quantitative constraints on paleo-BWO, combined with the $\Delta\delta^{13}C$, pore density, organic compound preservation, and aU data. The I/Ca proxy can be applied to regions, where epifaunal *Cibicidoides* spp. are present, but where there are no deep infaunal species for $\Delta\delta^{13}C$ calculation. Epifaunal I/Ca and pore density can provide confirmation of reconstructed $\Delta\delta^{13}C$ - BWO values. Given the complications and limitations of each proxy, we suggest that a multi-proxy approach is the best way forward, and low BWO con-

ditions (<50 μmol/kg) may be reliably detected, if more than one of the following are observed: low epifaunal I/Ca values (i.e., <~3 μmol/mol); low $\Delta\delta^{13}C$ (i.e., <~0.8‰); and high pore area percentages (i.e., >~15%) (Fig. 2).

5. Discussion: global compilations

5.1. Updating the global compilation of glacial BWO

We next combine our I/Ca records with a compilation of $\Delta\delta^{13}C$ data (9 sites) and C_{37} alkenone data (7 sites) to show broad temporal and spatial patterns in (semi-)quantitative BWO (Fig. 5, Table S3). In addition, we update a global compilation of sediment aU records (108 sites) (Table S3), from which we highlight sites with coupled higher aU and lower/similar productivity, indicative of lower BWO in the LGM than at present (Bradtmiller et al., 2010). Differences in aU values at sites exposed to the same water mass are likely caused by differences in diagenetic processes and/or sedimentation rates (Costa et al., 2018).

There are two key observations in this multi-proxy compilation (Fig. 5): (i) The four proxies are generally consistent in space and time, indicating that bottom waters experienced various degrees of glacial-time deoxygenation. (ii) The areal extent of low O_2 waters (< ~50 μmol/kg) was more extensive during the last glacial period than today, at water depths >1500–2000 m in the Atlantic and Pacific Oceans. ODP Site 849 (water depth 3800 m) in the EEP exhibits relatively small variability in I/Ca (~3–5 μmol/mol) throughout this low-resolution record. No aU peaks were found in downcore samples at ODP Site 849 (Pichat et al., 2004), but this does not exclude the possibility of deoxygenation because aU peaks can be removed by subsequent reoxygenation combined with intense bioturbation (Costa et al., 2018). The C_{37} alkenone records at four intermediate to deep EEP sites (water depths 1.4–3.1 km) were interpreted to indicate BWO below 50 μmol/kg during the last glacial period (Anderson et al., 2019). Thus, low O_2 waters may have expanded to as deep as 3.1 km in the EEP as recognized by the (semi-)quantitative methods applied to date, but we do not yet have reliable semi-quantitative information about the degree of deoxygenation in the deepest EEP (>3.1 km). Previous global compilations of qualitative BWO proxies have shown lower BWO during the LGM in the deepest parts (3–5 km) of the Atlantic, North Pacific, and Indian sector of the Southern Ocean from trace metal records (Jaccard and Galbraith, 2012), but more research is needed to quantitatively constrain glacial conditions in the deepest parts (≥4 km) of all oceans.

5.2. Drivers of deoxygenation in the glacial Atlantic vs. Pacific Oceans

The relative dominance of different drivers (ventilation, O_2 utilization, the temperature-dependent O_2 solubility effect) was unlikely to be identical across depths (shallow and deep circulation cells) and ocean basins (Pacific vs. Atlantic), in determining the spatial patterns in glacial-interglacial BWO changes (Fig. 5). Today, the deep ocean is less oxygenated in the Pacific than in the South Atlantic because of the significant aging of deep waters in the Pacific Ocean (Broecker and Peng, 1982). Ocean circulation reconstructions suggest stronger stratification and more sluggish deep circulation during the LGM in the Atlantic (Ferrari et al., 2014; Howe et al., 2016; Roberts et al., 2016), whereas arguments for (Basak et al., 2018; Du et al., 2018) and against (Hu and Piotrowski, 2018) reduced ventilation in the glacial deep Pacific have been made.

During the glacial, export production generally may have increased in the South Atlantic (Kohfeld et al., 2005). In the Sub-Antarctic Atlantic, north of the Antarctic Polar Front (APF), increased dust flux during glacial times was associated with iron fertilization and a strengthened biological pump (Martínez-García et al., 2014). On the other hand, export production decreased in the glacial equatorial and North Pacific (Costa et al., 2018, 2016; Kohfeld and Chase, 2011) (Fig. 5). In the equatorial Pacific, dust deposition was greater during glacial periods, but whether it was large enough to provide substantial iron fertilization remains controversial (Costa et al., 2016; Loveley et al., 2017; Murray et al., 2012; Winckler et al., 2016). In the Sub-Antarctic East Pacific and just south of the APF, both dust deposition and export production increased during glacials relative to interglacials (Lamy et al., 2014).

This set of proxy records (Fig. 5C) covers the broadly defined glacial period, when the drivers for changes in the Earth system established for the LGM should largely apply. For glacial oceans, these records (Fig. 5C) obviously do not yet resolve the extent of low BWO (<50 μmol/kg) globally, but they do show potential to generate a hypothesis for comparison with models of the glacial ocean circulation and associated biogeochemical parameters. For example, low BWO appeared more frequently in the intermediate-deep parts of the Pacific (1.4–3 km) than in the upper-intermediate depths in the Atlantic (<2 km). The glacial deoxygenation in the deep circulation cells in both the South Atlantic and Pacific Oceans (Fig. 5) likely was driven by ventilation changes or air-sea disequilibrium (Eggleston and Galbraith, 2018; Ferrari et al., 2014; Khatiwala et al., 2019; Rae et al., 2018; Stephens and Keeling, 2000). Global temperature change might have influenced whole-ocean oxygenation more through reduced ventilation, than through changes in O_2 solubility due to cooling. In the glacial Pacific Ocean, lower productivity and deoxygenation at intermediate-deep water depths (1.4–3 km) suggests that ventilation changes may have had a major impact on BWO. In contrast, the enhanced biological pump in the Atlantic and possibly shallower deoxygenation (<2 km) suggest that productivity might have played an important additional role in driving glacial deoxygenation (Fig. 5C). Ventilation and productivity thus might have differently affected deoxygenation in the two ocean basins. More (semi-)quantitative records are required to confirm this spatial pattern for modeling work to explore mechanistic explanations, such as changes in the westerlies, dust supply, changes in the remineralization depth/efficiency, the nature of ecosystem communities, circulation rate/water mass extent, and density structure of the ocean.

5.3. Implications for glacial ocean carbon storage

Glacial bottom water deoxygenation is commonly associated with increased storage of respired carbon in the deep ocean (e.g., Anderson et al. (2019); Bradtmiller et al. (2010); Cartapanis et al. (2016); Hoogakker et al. (2018); Hoogakker et al. (2015); Jacobel et al. (2020)). CO_2 is removed from the surface ocean by photosynthesis, and oceanic O_2 is consumed through the respiration of fixed organic carbon, with a CO_2:O_2 stoichiometry of 0.7 below 400 m (Anderson and Sarmiento, 1994), although air-sea disequilibrium could alter the relationship between dissolved oceanic O_2 and carbon storage (Ito and Follows, 2013; Khatiwala et al., 2019). The respired carbon storage or respiratory CO_2 concentrations in the glacial-time ocean were estimated on a regional scale by calculating the oxygen utilization (the difference between measured BWO and the saturated dissolved O_2 concentrations of the water mass at each salinity and potential temperature) and using approximate Redfield ratios for C_{org}/O_2 of 117/170 (e.g., Hoogakker et al., 2015; 2018; Anderson et al., 2019). In future work, more (semi-)quantitative glacial BWO data with higher spatial coverage, especially in the same water mass, will help improve such calculations on carbon storage globally and in each ocean basin.

Global analyses of modern seawater show that $\delta^{13}C$ of dissolved inorganic carbon is significantly correlated with deep water

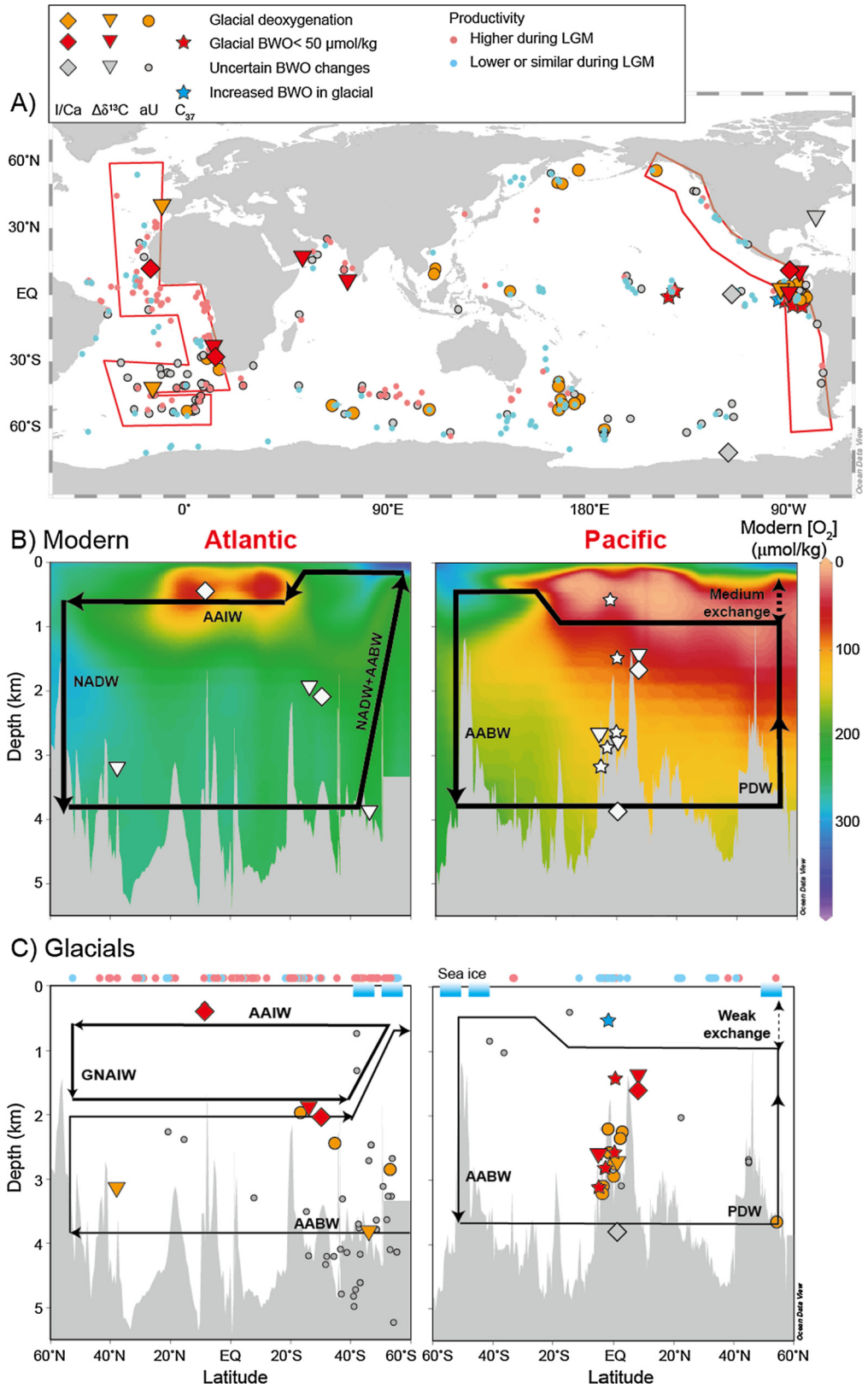

Fig. 5. Global compilation of benthic I/Ca, $\Delta\delta^{13}C$, C_{37} alkenones, and aU proxy records. (A) Map view, (B) modern and (C) glacial transects through the Atlantic and Pacific Oceans. Red symbols highlight sites with glacial deoxygenation and glacial BWO < 50 µmol/kg, as estimated from I/Ca < 3 µmol/mol, or an order-of-magnitude higher of C_{37} alkenones, or calculated from $\Delta\delta^{13}C$. "Uncertain" refers to sites without sufficient Holocene and/or glacial samples for I/Ca or $\Delta\delta^{13}C$ analyses and factors other than BWO hampering the interpretation of aU as BWO proxy, respectively. Note that the $\Delta\delta^{13}C$ calculated from *C. kullenbergi* at Sub-Antarctic Atlantic site MD07-3076Q (44.15°S, 14.23°W, 3.8 km) (Gottschalk et al., 2016a) has been re-calculated (Gottschalk et al., 2016b), because the calibration was only applicable for $\delta^{13}C_{C.\ wuellerstorfi}$. The productivity changes at the LGM relative to the late Holocene are adapted from Costa et al. (2017); Kohfeld et al. (2005). The ocean circulation in panel B and C is adapted from Du et al. (2018); Sigman et al. (2010). NADW: North Atlantic Deep Water; AABW: Antarctic Bottom Water; AAIW: Antarctic Intermediate Water; GNAIW: Glacial North Atlantic Intermediate Water; PDW: Pacific Deep Water.

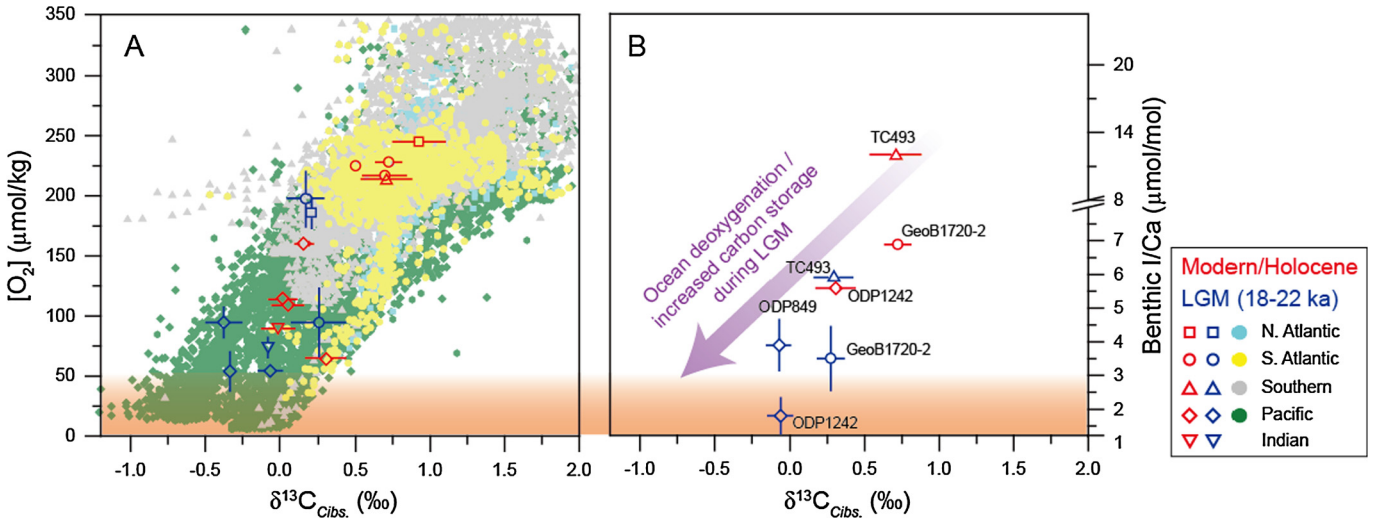

Fig. 6. A) Averaged *Cibicidoides* spp. $\delta^{13}C$ versus $[O_2]_{BW}$ and B) I/Ca at each site with down-core data between modern/Holocene and LGM (open symbols). The LGM $[O_2]$ values in panel A are derived from $\Delta\delta^{13}C$. Background scatter plot in panel A shows the modern global relationship between seawater $[O_2]$ and $\delta^{13}C$ of dissolved inorganic carbon based on seawater analyses (filled symbols) (Hoogakker et al., 2016). Red color band corresponds to $[O_2] < 50$ µmol/kg windows in Fig. 1B, and the *y*-axis are scaled to the proposed I/Ca - O_2 estimates discussed in the text. The arrows in panel B indicates the data trend towards decreased oxygenation and increased carbon storage in LGM. I/Ca values at site TC493 are not from the Holocene and the LGM but from MIS 5e and MIS 6.

O_2 (Hoogakker et al., 2016). Down-core records show similar positive relations between averaged $\delta^{13}C_{Cibicidoides}$ and I/Ca values or $\Delta\delta^{13}C$-derived O_2 estimates, supporting that bottom waters were overall less-oxygenated and carbon storage was higher during the LGM (Fig. 6). Our semi-quantitative BWO values thus agree with other observations that the glacial ocean was less well-ventilated and stored more respired carbon than the modern ocean, despite lower global temperatures. Climate-driven changes in ocean ventilation and biological productivity thus can outweigh the effect of temperature-dependent O_2 solubility in determining past ocean deoxygenation and may have played different roles in the glacial Atlantic vs. Pacific Oceans.

6. Conclusions

We document the potential of epifaunal I/Ca as a promising semi-quantitative BWO proxy, and demonstrate that epifaunal I/Ca combined with independent other proxies (e.g., $\Delta\delta^{13}C$ and pore area percentages) can provide more reliable reconstructions of BWO in the world ocean than the use of a single proxy. The global compilation of I/Ca, $\Delta\delta^{13}C$ and C_{37} alkenone records indicates that waters with $O_2 < 50$ µmol/kg were more extensive in the Atlantic and Pacific Oceans during glacial periods than present day, and that the driving mechanisms of glacial-time deoxygenation may have differed between ocean basins. Our results support a glacial ocean with generally less-oxygenated bottom waters at water depths >1500-2000 m and increased carbon storage.

Declaration of competing interest

The authors declare that they have no known competing financial interests or personal relationships that could have appeared to influence the work reported in this paper.

Acknowledgements

We thank Lamont-Doherty Core Repository for providing core-top materials, the Bremen GeoB core repository for curating and providing material from core GeoB1720-2. Enqing Huang and Jun Tian provided samples from GeoB9532-9535. We also thank Simona Nicoara at Open University for the $\delta^{18}O$ analysis at core GeoB1720-2. This study benefited from discussions with Robert F. Anderson. This work is supported by NSF grants OCE-1232620, OCE-1736542 and EAR-1349252 (to ZL), OCE 1736538 (to ET), OCE 10-60992 (to AR), NERC grant NE/I020563/1 (to BH), ERC Consolidator grant no: 681746 (to RR), and Syracuse University Graduate Fellowship and Research Excellence Doctoral Funding Fellowship (to WL).

Appendix A. Supplementary material

Supplementary material related to this article can be found online at https://doi.org/10.1016/j.epsl.2019.116055.

References

Anderson, L.A., Sarmiento, J.L., 1994. Redfield ratios of remineralization determined by nutrient data analysis. Glob. Biogeochem. Cycles 8, 65–80.
Anderson, R.F., Sachs, J.P., Fleisher, M.Q., Allen, K.A., Yu, J., Koutavas, A., Jaccard, S.L., 2019. Deep-sea oxygen depletion and ocean carbon sequestration during the last ice age. Glob. Biogeochem. Cycles 33, 1–17.
Barker, S., Greaves, M., Elderfield, H., 2003. A study of cleaning procedures used for foraminiferal Mg/Ca paleothermometry. Geochem. Geophys. Geosyst. 4.
Bartlett, R., Elrick, M., Wheeley, J.R., Polyak, V., Desrochers, A., Asmerom, Y., 2018. Abrupt global-ocean anoxia during the Late Ordovician–early Silurian detected using uranium isotopes of marine carbonates. Proc. Natl. Acad. Sci. 115, 5896–5901.
Basak, C., Fröllje, H., Lamy, F., Gersonde, R., Benz, V., Anderson, R.F., Molina-Kescher, M., Pahnke, K., 2018. Breakup of last glacial deep stratification in the South Pacific. Science 359, 900–904.
Boyer, T.P., Antonov, J.I., Baranova, O.K., Coleman, C., Garcia, H.E., Grodsky, A., Johnson, D.R., Locarnini, R.A., Mishonov, A.V., O'Brien, T.D., Paver, C.R., Reagan, J.R., Seidov, D., Smolyar, I.V., Zweng, M.M., 2013. World Ocean Database 2013, NOAA Atlas NESDIS 72. Silver Spring, MD. 209 p.
Bradtmiller, L., Anderson, R., Sachs, J., Fleisher, M., 2010. A deeper respired carbon pool in the glacial equatorial Pacific Ocean. Earth Planet. Sci. Lett. 299, 417–425.
Breitburg, D., Levin, L.A., Oschlies, A., Grégoire, M., Chavez, F.P., Conley, D.J., Garçon, V., Gilbert, D., Gutiérrez, D., Isensee, K., 2018. Declining oxygen in the global ocean and coastal waters. Science 359, eaam7240.
Broecker, W.S., Peng, T.H., 1982. Tracers in the Sea. Columbia University, Palisades, NY.
Cartapanis, O., Bianchi, D., Jaccard, S.L., Galbraith, E.D., 2016. Global pulses of organic carbon burial in deep-sea sediments during glacial maxima. Nat. Commun. 7, 10796.
Chance, R., Baker, A.R., Carpenter, L., Jickells, T.D., 2014. The distribution of iodide at the sea surface. Env. Sci. Process. Impacts 16, 1841–1859.
Costa, K.M., Anderson, R.F., McManus, J.F., Winckler, G., Middleton, J.L., Langmuir, C.H., 2018. Trace element (Mn, Zn, Ni, V) and authigenic uranium (aU) geochemistry reveal sedimentary redox history on the Juan de Fuca Ridge, North Pacific Ocean. Geochim. Cosmochim. Acta 236, 79–98.

Costa, K.M., Jacobel, A.W., McManus, J.F., Anderson, R.F., Winckler, G., Thiagarajan, N., 2017. Productivity patterns in the equatorial Pacific over the last 30,000 years. Glob. Biogeochem. Cycles 31, 850–865.

Costa, K.M., McManus, J.F., Anderson, R.F., Ren, H., Sigman, D., Winckler, G., Fleisher, M.Q., Marcantonio, F., Ravelo, A.C., 2016. No iron fertilization in the equatorial Pacific Ocean during the last ice age. Nature 529, 519.

Cutter, G.A., Moffett, J.G., Nielsdóttir, M.C., Sanial, V., 2018. Multiple oxidation state trace elements in suboxic waters off Peru: in situ redox processes and advective/diffusive horizontal transport. Mar. Chem. 201, 77–89.

de la Fuente, M., Calvo, E., Skinner, L., Pelejero, C., Evans, D., Müller, W., Povea, P., Cacho, I., 2017. The evolution of deep ocean chemistry and respired carbon in the Eastern Equatorial Pacific over the last deglaciation. Paleoceanography 32, 1371–1385.

Dickson, A.J., Beer, C.J., Dempsey, C., Maslin, M.A., Bendle, J.A., McClymont, E.L., Pancost, R.D., 2009. Oceanic forcing of the Marine Isotope Stage 11 interglacial. Nat. Geosci. 2, 428–433.

Du, J., Haley, B.A., Mix, A.C., Walczak, M.H., Praetorius, S.K., 2018. Flushing of the deep Pacific Ocean and the deglacial rise of atmospheric CO_2 concentrations. Nat. Geosci. 11, 749.

Durand, A., Chase, Z., Noble, T.L., Bostock, H., Jaccard, S.L., Townsend, A.T., Bindoff, N.L., Neil, H., Jacobsen, G., 2018. Reduced oxygenation at intermediate depths of the southwest Pacific during the last glacial maximum. Earth Planet. Sci. Lett. 491, 48–57.

Eggleston, S., Galbraith, E.D., 2018. The devil's in the disequilibrium: multi-component analysis of dissolved carbon and oxygen changes under a broad range of forcings in a general circulation model. Biogeosciences 15, 3761–3777.

Farrenkopf, A.M., Luther, G.W., 2002. Iodine chemistry reflects productivity and denitrification in the Arabian Sea: evidence for flux of dissolved species from sediments of western India into the OMZ. Deep-Sea Res., Part 2, Top. Stud. Oceanogr. 49, 2303–2318.

Feng, X., Redfern, S.A., 2018. Iodate in calcite, aragonite and vaterite $CaCO_3$: insights from first-principles calculations and implications for the I/Ca geochemical proxy. Geochim. Cosmochim. Acta 236, 351–360.

Ferrari, R., Jansen, M.F., Adkins, J.F., Burke, A., Stewart, A.L., Thompson, A.F., 2014. Antarctic sea ice control on ocean circulation in present and glacial climates. Proc. Natl. Acad. Sci. 201323922.

Glock, N., Liebetrau, V., Eisenhauer, A., 2014. I/Ca ratios in benthic foraminifera from the Peruvian oxygen minimum zone: analytical methodology and evaluation as proxy for redox conditions. Biogeosciences (BG) 11, 7077–7095.

Gottschalk, J., Skinner, L.C., Lippold, J., Vogel, H., Frank, N., Jaccard, S.L., Waelbroeck, C., 2016a. Biological and physical controls in the Southern Ocean on past millennial-scale atmospheric CO_2 changes. Nat. Commun. 7, 11539.

Gottschalk, J., Vázquez Riveiros, N., Waelbroeck, C., Skinner, L.C., Michel, E., Duplessy, J.C., Hodell, D., Mackensen, A., 2016b. Carbon isotope offsets between benthic foraminifer species of the genus Cibicides (Cibicidoides) in the glacial sub-Antarctic Atlantic. Paleoceanogr. Paleoclimatol. 31, 1583–1602.

Gruber, N., Gloor, M., Fan, S.M., Sarmiento, J.L., 2001. Air-sea flux of oxygen estimated from bulk data: implications for the marine and atmospheric oxygen cycles. Glob. Biogeochem. Cycles 15, 783–803.

Hedges, J.I., Keil, R.G., 1995. Sedimentary organic matter preservation: an assessment and speculative synthesis. Mar. Chem. 49, 81–115.

Hoogakker, B., Lu, Z., Umling, N., Jones, L., Zhou, X., Rickaby, R., Thunell, R., Cartapanis, O., Galbraith, E.D., 2018. Glacial expansion of oxygen-depleted seawater in the eastern tropical Pacific. Nature 562, 410–413.

Hoogakker, B., Thornalley, D., Barker, S., 2016. Millennial changes in North Atlantic oxygen concentrations. Biogeosciences 13, 211–221.

Hoogakker, B.A., Elderfield, H., Schmiedl, G., McCave, I.N., Rickaby, R.E., 2015. Glacial-interglacial changes in bottom-water oxygen content on the Portuguese margin. Nat. Geosci. 8, 40.

Howe, J.N., Piotrowski, A.M., Noble, T.L., Mulitza, S., Chiessi, C.M., Bayon, G., 2016. North Atlantic deep water production during the last glacial maximum. Nat. Commun. 7, 11765.

Hu, R., Piotrowski, A.M., 2018. Neodymium isotope evidence for glacial-interglacial variability of deepwater transit time in the Pacific Ocean. Nat. Commun. 9, 4709.

Huang, E., Mulitza, S., Paul, A., Groeneveld, J., Steinke, S., Schulz, M., 2012. Response of eastern tropical Atlantic central waters to Atlantic meridional overturning circulation changes during the Last Glacial Maximum and Heinrich Stadial 1. Paleoceanography 27, PA3229.

Huang, Z., Ito, K., Morita, I., Yokota, K., Fukushi, K., Timerbaev, A.R., Watanabe, S., Hirokawa, T., 2005. Sensitive monitoring of iodine species in sea water using capillary electrophoresis: vertical profiles of dissolved iodine in the Pacific Ocean. J. Environ. Monit. 7, 804–808.

Ito, T., Follows, M.J., 2013. Air-sea disequilibrium of carbon dioxide enhances the biological carbon sequestration in the Southern Ocean. Glob. Biogeochem. Cycles 27, 1129–1138.

Jaccard, S.L., Galbraith, E.D., 2012. Large climate-driven changes of oceanic oxygen concentrations during the last deglaciation. Nat. Geosci. 5, 151.

Jaccard, S.L., Galbraith, E.D., Martínez-García, A., Anderson, R.F., 2016. Covariation of deep Southern Ocean oxygenation and atmospheric CO_2 through the last ice age. Nature 530, 207.

Jacobel, A.W., Anderson, R., Jaccard, S.L., McManus, J., Pavia, F.J., Winckler, G., 2020. Deep Pacific storage of respired carbon during the last ice age: perspectives from bottom water oxygen reconstructions. Quat. Sci. Rev. https://doi.org/10.1016/j.quascirev.2019.106065. In press.

Jacobel, A.W., Winckler, G., McManus, J., Anderson, R., 2017. Repeated storage of respired carbon in the equatorial Pacific Ocean over the last three glacial cycles. Nat. Commun. 8, 1727.

Jenkyns, H.C., 2010. Geochemistry of oceanic anoxic events. Geochem. Geophys. Geosyst. 11, Q03004.

Jorissen, F.J., Fontanier, C., Thomas, E., 2007. Chapter seven paleoceanographical proxies based on deep-sea benthic foraminiferal assemblage characteristics. Develop. Mar. Geol. 1, 263–325.

Kaiho, K., 1994. Benthic foraminiferal dissolved-oxygen index and dissolved-oxygen levels in the modern ocean. Geology 22, 719–722.

Keeling, R.F., Körtzinger, A., Gruber, N., 2009. Ocean deoxygenation in a warming world. Annu. Rev. Mar. Sci. 2, 199–229.

Khatiwala, S., Schmittner, A., Muglia, J., 2019. Air-sea disequilibrium enhances ocean carbon storage during glacial periods. Sci. Adv. 5, eaaw4981.

Kohfeld, K.E., Chase, Z., 2011. Controls on deglacial changes in biogenic fluxes in the North Pacific Ocean. Quat. Sci. Rev. 30, 3350–3363.

Kohfeld, K.E., Le Quéré, C., Harrison, S.P., Anderson, R.F., 2005. Role of marine biology in glacial-interglacial CO_2 cycles. Science 308, 74–78.

Kuhnt, T., Schiebel, R., Schmiedl, G., Milker, Y., Mackensen, A., Friedrich, O., 2014. Automated and manual analyses of the pore density-to-oxygen relationship in Globobulimina turgida (Bailey). J. Foraminiferal Res. 44, 5–16.

Lamy, F., Gersonde, R., Winckler, G., Esper, O., Jaeschke, A., Kuhn, G., Ullermann, J., Martínez-Garcia, A., Lambert, F., Kilian, R., 2014. Increased dust deposition in the Pacific Southern Ocean during glacial periods. Science 343, 403–407.

Loubere, P., Gary, A., 1990. Taphonomic process and species microhabitats in the living to fossil assemblage transition of deeper water benthic foraminifera. Palaios 5, 375–381.

Loveley, M.R., Marcantonio, F., Wisler, M.M., Hertzberg, J.E., Schmidt, M.W., Lyle, M., 2017. Millennial-scale iron fertilization of the eastern equatorial Pacific over the past 100,000 years. Nat. Geosci. 10, 760–764.

Lu, W., Dickson, A.J., Thomas, E., Rickaby, R., Chapman, P., Lu, Z., 2019. Refining the planktic foraminiferal I/Ca proxy: results from the Southeast Atlantic Ocean. Geochim. Cosmochim. Acta. https://doi.org/10.1016/j.gca.2019.1010.1025. In press.

Lu, W., Ridgwell, A., Thomas, E., Hardisty, D.S., Luo, G., Algeo, T.J., Saltzman, M.R., Gill, B.C., Shen, Y., Ling, H.-F., Edwards, C.T., Whalen, M.T., Zhou, X., Gutchess, K.M., Jin, L., Rickaby, R., Jenkyns, H.C., Lyons, T.W., Lenton, T.M., Kump, L., Lu, Z., 2018. Late inception of a resiliently oxygenated upper ocean. Science 361, 174–177.

Lu, Z., Hoogakker, B.A., Hillenbrand, C.-D., Zhou, X., Thomas, E., Gutchess, K.M., Lu, W., Jones, L., Rickaby, R.E., 2016. Oxygen depletion recorded in upper waters of the glacial Southern Ocean. Nat. Commun. 7.

Lu, Z., Jenkyns, H.C., Rickaby, R.E., 2010. Iodine to calcium ratios in marine carbonate as a paleo-redox proxy during oceanic anoxic events. Geology 38, 1107–1110.

Lutze, G., Thiel, H., 1989. Epibenthic foraminifera from elevated microhabitats; Cibicidoides wuellerstorfi and Planulina ariminensis. J. Foraminiferal Res. 19, 153–158.

Mackensen, A., Hubberten, H.W., Bickert, T., Fischer, G., Fütterer, D., 1993. The δ13C in benthic foraminiferal tests of Fontbotia wuellerstorfi (Schwager) relative to the δ13C of dissolved inorganic carbon in southern ocean deep water: implications for glacial ocean circulation models. Paleoceanography 8, 587–610.

Martínez-García, A., Sigman, D.M., Ren, H., Anderson, R.F., Straub, M., Hodell, D.A., Jaccard, S.L., Eglinton, T.I., Haug, G.H., 2014. Iron fertilization of the Subantarctic Ocean during the last ice age. Science 343, 1347–1350.

McCorkle, D.C., Emerson, S.R., 1988. The relationship between pore water carbon isotopic composition and bottom water oxygen concentration. Geochim. Cosmochim. Acta 52, 1169–1178.

McKay, C., Filipsson, H., Romero, O., Stuut, J.B., Björck, S., 2016. The interplay between the surface and bottom water environment within the Benguela upwelling system over the last 70 ka. Paleoceanography 31, 266–285.

Murray, R.W., Leinen, M., Knowlton, C.W., 2012. Links between iron input and opal deposition in the Pleistocene equatorial Pacific Ocean. Nat. Geosci. 5, 270.

Oschlies, A., Brandt, P., Stramma, L., Schmidtko, S., 2018. Drivers and mechanisms of ocean deoxygenation. Nat. Geosci. 1.

Oschlies, A., Duteil, O., Getzlaff, J., Koeve, W., Landolfi, A., Schmidtko, S., 2017. Patterns of deoxygenation: sensitivity to natural and anthropogenic drivers. Philos. Trans. R. Soc. Ser. A 375, 20160325.

Penn, J.L., Deutsch, C., Payne, J.L., Sperling, E.A., 2018. Temperature-dependent hypoxia explains biogeography and severity of end-Permian marine mass extinction. Science 362, eaat1327.

Pichat, S., Sims, K.W., François, R., McManus, J.F., Brown Leger, S., Albarède, F., 2004. Lower export production during glacial periods in the equatorial Pacific derived from (^{231}Pa/^{230}Th) xs, 0 measurements in deep-sea sediments. Paleoceanogr. Paleoclimatol. 19.

Podder, J., Lin, J., Sun, W., Botis, S., Tse, J., Chen, N., Hu, Y., Li, D., Seaman, J., Pan, Y., 2017. Iodate in calcite and vaterite: insights from synchrotron X-ray absorption

spectroscopy and first-principles calculations. Geochim. Cosmochim. Acta 198, 218–228.
Rae, J., Burke, A., Robinson, L., Adkins, J., Chen, T., Cole, C., Greenop, R., Li, T., Littley, E., Nita, D., 2018. CO_2 storage and release in the deep Southern Ocean on millennial to centennial timescales. Nature 562, 569.
Rathburn, A., Miao, Q., 1995. The taphonomy of deep-sea benthic foraminifera: comparisons of living and dead assemblages from □ and gravity cores taken in the Sulu Sea. Mar. Micropaleontol. 25, 127–149.
Rathburn, A.E., Corliss, B.H., 1994. The ecology of living (stained) deep-sea benthic foraminifera from the Sulu Sea. Paleoceanography 9, 87–150.
Rathburn, A.E., Willingham, J., Ziebis, W., Burkett, A.M., Corliss, B.H., 2018. A new biological proxy for deep-sea paleo-oxygen: pores of epifaunal benthic foraminifera. Sci. Rep. 8, 9456.
Resplandy, L., 2018. Will ocean zones with low oxygen levels expand or shrink? Nature 557, 314–315.
Roberts, J., Gottschalk, J., Skinner, L.C., Peck, V.L., Kender, S., Elderfield, H., Waelbroeck, C., Riveiros, N.V., Hodell, D.A., 2016. Evolution of South Atlantic density and chemical stratification across the last deglaciation. Proc. Natl. Acad. Sci. 113, 514–519.
Rue, E.L., Smith, G.J., Cutter, G.A., Bruland, K.W., 1997. The response of trace element redox couples to suboxic conditions in the water column. Deep-Sea Res., Part 1, Oceanogr. Res. Pap. 44, 113–134.
Schmidtko, S., Stramma, L., Visbeck, M., 2017. Decline in global oceanic oxygen content during the past five decades. Nature 542, 335–339.
Schweizer, M., Pawlowski, J., Kouwenhoven, T., van der Zwaan, B., 2009. Molecular phylogeny of common cibicidids and related Rotaliida (Foraminifera) based on small subunit rDNA sequences. J. Foraminiferal Res. 39, 300–315.
Sigman, D.M., Hain, M.P., Haug, G.H., 2010. The polar ocean and glacial cycles in atmospheric CO_2 concentration. Nature 466, 47.
Song, H., Song, H., Algeo, T.J., Tong, J., Romaniello, S.J., Zhu, Y., Chu, D., Gong, Y., Anbar, A.D., 2017. Uranium and carbon isotopes document global-ocean redox-productivity relationships linked to cooling during the Frasnian-Famennian mass extinction. Geology 45, 887–890.
Stephens, B.B., Keeling, R.F., 2000. The influence of Antarctic sea ice on glacial–interglacial CO_2 variations. Nature 404, 171.
Stramma, L., Oschlies, A., Schmidtko, S., 2012. Mismatch between observed and modeled trends in dissolved upper-ocean oxygen over the last 50 yr. Biogeosciences (BG) 9, 4045–4057.
Umling, N.E., Thunell, R.C., 2018. Mid-depth respired carbon storage and oxygenation of the eastern equatorial Pacific over the last 25,000 years. Quat. Sci. Rev. 189, 43–56.
Venturelli, R.A., Rathburn, A., Burkett, A., Ziebis, W., 2018. Epifaunal foraminifera in an infaunal world: insights into the influence of heterogeneity on the Benthic ecology of oxygen-poor, deep-sea habitats. Front. Mar. Sci. 5, 344.
Winckler, G., Anderson, R.F., Jaccard, S.L., Marcantonio, F., 2016. Ocean dynamics, not dust, have controlled equatorial Pacific productivity over the past 500,000 years. Proc. Natl. Acad. Sci. 113, 6119–6124.
Wollenburg, J.E., Zittier, Z.M., Bijma, J., 2018. Insight into deep-sea life–Cibicidoides pachyderma substrate and pH-dependent behaviour following disturbance. Deep-Sea Res., Part 1, Oceanogr. Res. Pap. 138, 34–45.
Wong, G.T., Brewer, P.G., 1977. The marine chemistry of iodine in anoxic basins. Geochim. Cosmochim. Acta 41, 151–159.
Zhou, X., Thomas, E., Rickaby, R.E., Winguth, A.M., Lu, Z., 2014. I/Ca evidence for upper ocean deoxygenation during the PETM. Paleoceanography 29, 964–975.
Zou, K.H., O'Malley, J., Mauri, L., 2007. Receiver-operating characteristic analysis for evaluating diagnostic tests and predictive models. Circulation 115, 654–657.